

## Time Evolution of Freely Expanded Bose-Einstein Condensates Containing Small Numbers of Atoms

De-Sheng Hong,<sup>1</sup> K. H. Huang,<sup>1</sup> Tsin-Fu Jiang,<sup>2</sup> and D. J. Han<sup>1,\*</sup>

<sup>1</sup>*Department of Physics, National Chung Cheng University, Chia-Yi 621, Taiwan, R. O. C.*

<sup>2</sup>*Institute of Physics, National Chiao Tung University, Hsinchu 300, Taiwan, R. O. C.*

(Received October 4, 2006)

We investigate the time evolution of freely expanded Bose-Einstein condensates by measuring their aspect ratios at different times after their release from a magnetic trap. In these measurements the condensates contain no more than 9000 <sup>87</sup>Rb atoms. By varying the trapping frequency and atom number, we measure the condensate aspect ratios at different expansion times in free space. We compare our measurements with those calculated from the Thomas-Fermi model and a direct numerical solution. Under our trapping condition, the data of the time dependent aspect ratios of the freely expanded condensates reasonably agrees with the numerical calculations, but shows a clear deviation from the predictions of the Thomas-Fermi model when the atom number in the condensates is small.

PACS numbers: 32.80.Pj, 03.75.Kk, 05.30.Jp

The achievement of a Bose-Einstein condensation (BEC) of dilute alkaline atoms in magnetic traps [1–3] provides an unprecedented opportunity for studying the physics in many fields [4]. The dilute atomic condensate is well described by the nonlinear Gross-Pitaevskii (GP) equation [5]. A GP equation contains the kinetic energy, the trap potential, and the mean-field energy, which is proportional to the local density of the condensate and plays a fundamental role in its dynamics. One of the special features in the experiments of trapped atomic condensates is that the trapping condition can be tuned on a time scale comparable to the atomic oscillation period. This provides the system with good test conditions for studying the time-dependent dynamics of the condensates either in or out of a trap.

Many investigations of the condensate dynamics are mostly on collective excitations, vortices generation, and sound speed measurements [6–9]. Those measurements are carried out with high precision, thereby allowing for a detailed comparison with theory. Measurements on the time evolution of an untrapped condensate, such as in a free space, is another important and interesting topic of investigation. One of the key parameters for describing an expanding condensate is its aspect ratio  $\sigma$ , which is normally defined as a ratio of the condensate widths along the two symmetric axes. For the magnetic TOP trap [10] that we use in this experiment the axes are parallel to the axial and the radial direction, respectively. Not only does this measurement show the first convincing evidence for a distinction between a thermal cloud and a condensate, it is also a direct test of the validity of the GP equation when applied to a dilute atomic sample in the degenerate regime.

The early studies of measuring the free-falling condensate aspect ratio were mostly on those with atom number  $N \geq 10^5$  [2, 11–13]. Their measurements prove that the TF

approximation is valid for condensates consisting of large atom numbers. Only a few groups worked on condensates with  $N \ll 10^5$  [1, 14, 15]. In this extreme regime with small atom numbers, the TF model turned out to be unsuitable.

In this paper, we present our measurements on the  $^{87}\text{Rb}$  condensate aspect ratio evolution with time in free space. Both the trapping frequency and atom number are allowed to vary. The experimental conditions are set to right around the transition border between the two extreme regimes where the previous investigations were carried out. We observe clear evidence that the Thomas-Fermi approximation begins to fail as the atom number is gradually lowered from  $N = 9000$  to  $3000$  under our trapping condition.

The dynamics of a condensate of  $N$  atoms in a trap potential  $U(\mathbf{r})$  can be well understood by examining the Gross-Pitaevskii equation at a time  $t$ ,

$$\left[ -\frac{\hbar^2}{2m}\nabla^2 + U(\mathbf{r}, t) + Ng|\psi(\mathbf{r}, t)|^2 \right] \psi(\mathbf{r}, t) = \mu\psi(\mathbf{r}, t), \quad (1)$$

where  $m$  is the atomic mass,  $\mu$  is the chemical potential,  $a$  is the s-wave scattering length,  $g = 4\pi\hbar^2 a/m$ , and  $\psi(\mathbf{r}, t)$  is the condensate wave function normalized as  $\int \psi(\mathbf{r}, t)^2 d\mathbf{r} = 1$ . The term  $Ng|\psi(\mathbf{r}, t)|^2$  represents the mean-field energy. To model the free expansion of a condensate, the trap potential is suddenly switched off at a certain time, say  $t = 0$ , and thus  $U(\mathbf{r}, t) = 0$  as  $t \geq 0$ . Substituting this potential into the GP equation should allow one to solve the condensate wavefunction for  $t > 0$  as in free expansion, if its spatial distribution is known at the moment the trap is turned off.

Some studies on direct numerical solution of the time dependent GP equation for the macroscopic wave function of the condensate were carried out [16, 17]. However, an analytical solution of the nonlinear GP equation will certainly be more beneficial, allowing a lucid description of the condensate dynamics and an immediate comparison with experiment. In a situation when the condensate arrives at the so-called Thomas-Fermi (TF) regime, the kinetic energy term is much smaller than the mean-field energy and can be neglected in Eq. (1) [18]. Under this condition the GP equation is simplified and allows one to solve for  $\psi(\mathbf{r})$  directly. As long as  $\mu \geq U(\mathbf{r}, t)$ , the result is

$$\psi_{TF}(\mathbf{r}, t) = \left[ \frac{\mu - U(\mathbf{r}, t)}{Ng} \right]^{1/2}. \quad (2)$$

Otherwise,  $\psi_{TF}(\mathbf{r}, t)$  is 0. For a harmonic potential  $U(\mathbf{r}, t) = \frac{1}{2}m[\omega_x^2(t)x^2 + \omega_y^2(t)y^2 + \omega_z^2(t)z^2]$ , the chemical potential is determined by the normalization of  $\psi_{TF}$ :

$$\mu_{TF} = \frac{1}{2}\hbar\bar{\omega} \left( 15Na\sqrt{\frac{m\bar{\omega}}{\hbar}} \right)^{2/5}, \quad (3)$$

where  $\bar{\omega} = [\omega_x(0)\omega_y(0)\omega_z(0)]^{1/3}$  is the geometric mean of the oscillation frequencies.

A simple model showing the validity of the TF approximation is described in Ref. [19]. For simplification, we here ignore the time variable  $t$ . To a good approximation, we

can assume an isotropic harmonic trapping potential  $U(\mathbf{r}) = \frac{1}{2}m(\omega^2x^2 + \omega^2y^2 + \omega^2z^2)$ , and then take the trial function of a Gaussian shape  $\psi = Ae^{-r^2/2b^2}$  into the GP equation and obtain the energy as

$$E = \frac{3}{4}\hbar\omega \left( \frac{a_{ho}^2}{b^2} + \frac{b^2}{a_{ho}^2} \right) + \frac{Ng}{(2\pi)^{3/2}} \frac{1}{b^3}, \quad (4)$$

where  $a_{ho} = \sqrt{\frac{\hbar}{m\omega}}$  is the characteristic radius of the Gaussian ground-state wavefunction. In Eq. (4) the ratio of the mean field energy to the kinetic energy is  $\alpha \sim \frac{Na}{a_{ho}}$ . If  $g > 0$  and  $\alpha \gg 1$ , namely

$$N \gg \frac{a_{ho}}{a}, \quad (5)$$

the kinetic energy is negligible. Eq. (5) then sets a general criterion for a system if the TF approximation is suitable. For the case of the  $^{87}\text{Rb}$  atom, the s-wave scattering length for the trapped state  $5^2S_{1/2}$ ,  $|F=2, M_F=2\rangle$ , is  $a \sim 5.3$  nm [20], and a trap with oscillation frequency  $\omega/2\pi = 13$  Hz, as that in our experiment, has  $a_{ho} \sim 2.8$   $\mu\text{m}$ . This requires the atom number  $N \gg 600$  to reach the TF regime. Most of the previous measurements on the freely expanded condensates are in this regime, except those shown in Refs. [1, 14, 15]. Our experimental condition, with the trap frequencies  $\omega/2\pi \sim 13$  Hz and  $N$  varying from 3000 atoms to 9000 atoms, is indeed in a regime where the criterion shown in Eq. (5) is not fully satisfied.

Castin and Dum developed a useful and straightforward way to apply the TF model on the condensate evolution in a time-dependent potential [21]. In order to compare our data with that obtained from the TF approximation, we use their calculation theory. Here we briefly outline their model by following the notations in Ref. [21]. The spatial density of a condensate of  $N$  atoms at a time  $t$  is  $\rho(\mathbf{r}, t) = N\psi_{TF}(\mathbf{r}, t)^2$ . Assume the trap is suddenly switched off at  $t = 0$ , the corresponding spatial density distribution is  $\rho(\mathbf{r}, 0)$ . Introducing scaling factors in the three axes  $\lambda_j(t)$ ,  $j = 1, 2, 3$ , which satisfy the equation

$$\ddot{\lambda}_j = \frac{\omega_j^2(0)}{\lambda_j\lambda_1\lambda_2\lambda_3} - \omega_j^2(t)\lambda_j, \quad (j = 1, 2, 3), \quad (6)$$

the spatial density evolves as

$$\rho(\mathbf{r}, t) = \frac{1}{\lambda_1(t)\lambda_2(t)\lambda_3(t)} \rho\left[\left\{r_j/\lambda_j(t)\right\}_{j=1,2,3}, 0\right]. \quad (7)$$

When applying this model to the condensate of  $^{87}\text{Rb}$  atoms in our magnetic TOP trap, we assume  $\omega_1(t) = \omega_2(t) = \omega_r(t)$  and  $\omega_3(t) = \omega_z(t)$ , where  $\omega_r(t)$  and  $\omega_z(t)$  are the radial and axial frequency, respectively. The scaling factors  $\lambda_1 = \lambda_2 \equiv \lambda_r$  and  $\lambda_3 \equiv \lambda_z$  in Eq. (7) evolve like

$$\frac{d^2}{d\tau^2} \lambda_r = \frac{1}{\lambda_r^3 \lambda_z}, \quad (8)$$

$$\frac{d^2}{d\tau^2} \lambda_z = \frac{\epsilon^2}{\lambda_r^2 \lambda_z^2}, \quad (9)$$

where  $\epsilon = \omega_z(0)/\omega_r(0)$  is known as the trap aspect ratio and  $\tau = \omega_r(0)t$ . At the expansion time  $t$  the aspect ratio  $\sigma(t)$  for a condensate is given by

$$\sigma(t) \equiv \frac{W_z(t)}{W_r(t)} = \frac{\lambda_z(t) \sqrt{2\mu_{TF}/m\omega_z^2(0)}}{\lambda_r(t) \sqrt{2\mu_{TF}/m\omega_r^2(0)}} = \frac{\lambda_z(t)}{\lambda_r(t)} \frac{1}{\epsilon}, \quad (10)$$

where  $W_z(t)$  and  $W_r(t)$  are the condensate size in the axial and radial directions, respectively. To calculate the time dependent aspect ratio  $\sigma(t)$ , we take the experimental parameters into Eqs. (8) and Eq. (9) to solve for  $\lambda_r(t)$  and  $\lambda_z(t)$  numerically.

The details of our experimental setup and procedure to produce Bose condensates have been published elsewhere [22]. Briefly, we first capture  $^{87}\text{Rb}$  atoms from a dispenser into the first MOT of our double MOT system. We capture about  $1 \times 10^9$  Rb atoms in 40 seconds. After molasses cooling and optical pumping the atoms in the state  $5S_{1/2}$ ,  $|F=2, M_F=2\rangle$  are transferred into the magnetic TOP trap. Our TOP trap consists of a pair of quadrupole coils and two pairs of rotating bias coils. The rotating frequency of the bias magnetic field is 9 kHz. Once the atoms are loaded, they are compressed and further cooled by rf evaporative cooling to the BEC border. After the BEC is formed, the rf is still left on and is fine tuned to produce a pure condensate containing a certain atom number between 3000 and 9000. We then adiabatically lower the quadrupole field gradient, while keeping the bias field fixed, to the value that the desired trap frequency is reached.

The cloud temperature in the decompressed TOP trap is less than 100 nK. The condensed atoms first sit in the weak trap for about 500 ms for equilibrium and are released by suddenly switching off the trap. The trap switch-off time is less than 200  $\mu\text{s}$  and is much shorter than the trap oscillation period. The released cloud is ballistically expanded in the free space and falls because of the gravity. We wait for an expansion time and shine an absorption probe beam of a duration time typically from 50 to 150  $\mu\text{s}$  into the BEC cloud for imaging.

The probe laser beam is close to the resonance frequency from the  $5S_{1/2}$ ,  $F=2$  to  $5P_{3/2}$ ,  $F'=3$  transition, and has the intensity of  $\sim 0.1I_s$ , where  $I_s$  is the saturation intensity for the  $F=2$ ,  $M_F=2$  to  $F'=3$ ,  $M_{F'}=3$  transition. The shadow of the BEC cloud is imaged onto a digital CCD camera for analysis. The typical image and spatial distribution of the expanded condensate cloud containing 9000 atoms at an expansion time of 18 ms are shown in Fig. 1.

The TOP trap potential for an atom of mass  $m$  is  $U(r, z) = \frac{1}{2}(m\omega_r^2 r^2 + m\omega_z^2 z^2)$ . The axial direction of our TOP trap is parallel to the  $z$  axis, and is along the direction of the gravitational force. If gravity is small compared to the trapping force, the trap aspect ratio  $\epsilon = \sqrt{8}$ , as in the typical TOP trap. However, gravity may play an important role on the TOP trap frequencies when the trap confinement is weak. Under this condition, the axial magnetic force  $M_F \mu_B B'_z$  is comparable to that required to levitate the atoms against the gravitational force  $mg$ , where  $\mu_B$  is the Bohr magneton,  $B'_z$  is the magnetic gradient in the axial direction, and  $g$  is the gravitational acceleration [23]. In general, taking the gravity

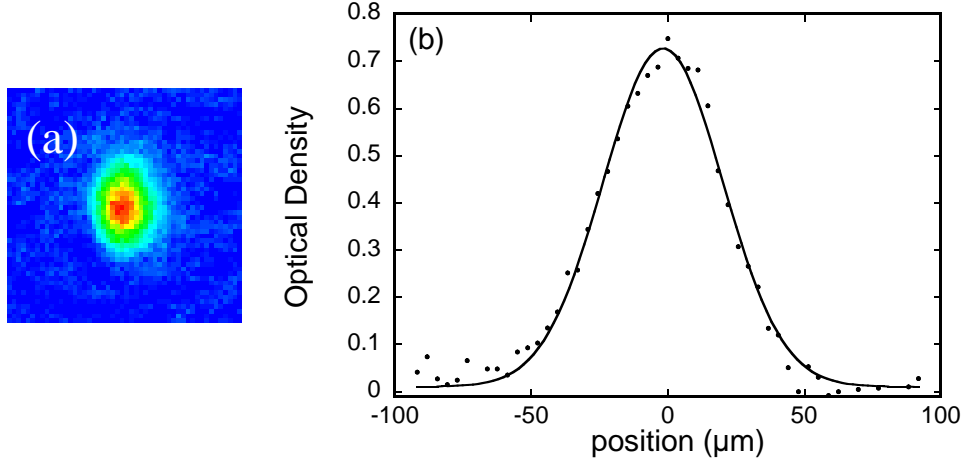


FIG. 1: Time-of-flight image of the pure condensate with  $N = 9000$ . (a)  $200 \mu\text{m} \times 200 \mu\text{m}$  false-color absorption images of pure condensates released from the TOP trap after a free expansion time of 18 ms. The vertical direction is aligned with the symmetry axis of the TOP trap and is in parallel with the gravitational force. (b) One-dimensional cuts through the center of the clouds, showing optical density vs horizontal position, for the image (a).

effect into account, the trapping frequencies of a TOP trap should be corrected as

$$\omega_r = \left( \frac{1}{\sqrt{8}} \right) \left( \frac{M_F \mu_B B_z'^2}{m B_b} \right)^{1/2} (1 + \eta^2)^{1/2} (1 - \eta^2)^{1/4} \quad (11)$$

and

$$\omega_z = \left( \frac{M_F \mu_B B_z'^2}{m B_b} \right)^{1/2} (1 - \eta^2)^{3/4}, \quad (12)$$

where  $B_b$  is the TOP bias field, and  $\eta = \frac{mg}{M_F \mu_B B_z'}$ . In this experiment the trapping potential is weak enough that the gravity effect sets in, thus  $\eta$  is  $\sim 0.25$  to  $0.28$  and  $\epsilon$  is no longer  $\sqrt{8}$ , but  $\sqrt{7.1}$  to  $\sqrt{6.83}$  instead.

The aspect ratio of a condensate strongly depends on the trap frequencies. Before the TOP trap was installed, we carefully calibrated its axial magnetic field gradient and bias field as  $B_z^{cal'}$  and  $B_b^{cal}$ . This allows us to calculate the trap frequencies to errors less than a few percent. One of the most precise ways to measure the trap frequencies is to directly monitor its center-of-mass position oscillation. This is carried out by first placing the atoms off-center with respect to the minimum of the trap potential for few milliseconds. The cloud then comes back towards the trap center and oscillates. Recording the center of mass positions of the cloud at different times allows us to measure the oscillation frequencies to very high accuracy.

We do the trapping frequency measurement using a cloud close to condensation. The trapped atoms are initially placed off-center in the axial direction while the axial magnetic

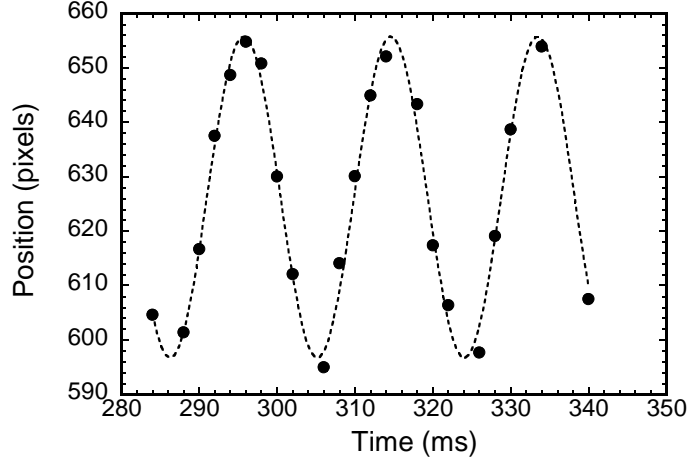


FIG. 2: TOP trap frequency measurement. The cloud center-of-mass position in the axial direction is plotted versus time. This measurement is done at the TOP trap condition with  $B_z^{cal'} = 92.56$  G/cm and  $B_b^{cal} = 4.25$  G. The experimental data are fitted with a sinusoidal function and give the trap oscillation period 188.85 ms, corresponding to an axial frequency  $\omega_z^{Exp} = 2\pi \times 52.95$  Hz.

field gradient  $B_z^{cal'}$  is 92.56 G/cm and the bias field  $B_b^{cal}$  equals 4.25 G. The measured cloud center position versus time is plotted in Fig. 2, in which the data points are fitted with a sinusoidal curve for a harmonic oscillation. The measured data indicate the axial oscillation frequency  $\omega_z^{Exp} = 2\pi \times 52.95$  Hz. The theoretical trap frequency  $\omega_z^{Th} = 2\pi \times 56.0$  Hz is calculated by Eq. (12) using the independently calibrated values  $B_z^{cal'}$  and  $B_b^{cal}$ . The measured frequency is 5.8% smaller than the theoretical value.

We attribute the discrepancy between the measured and theoretical values to the overestimate of the quadrupole field gradient for the following reasons. The rotating bias field of our TOP trap is generated by two pairs of coils, each with diameter  $\sim 12$  cm. They produce a rather uniform magnetic field over the whole trapping region. The bias field is well calibrated by a Gaussmeter and independently measured from the induced AC voltage across a pick-up coil. We believe the error from the bias field calibration is rather small and thus  $B_b = B_b^{cal}$ . However, measurement of the magnetic field gradient is very sensitive to the position where the Gaussmeter probe is located. Furthermore, the trap oscillation frequencies depend linearly on  $B_z'$  but on the square root of  $B_b$ . Therefore the true axial field gradient  $B_z^{T'}$  is inferred by lowering the pre-calibrated  $B_z^{cal'}$  by 5.8%. The trap frequencies used in the GP equation are calculated by taking the bias field  $B_b^{cal}$  and the corrected axial field gradient  $B_z^{T'}$  into Eqs. (11) and (12).

Our measurements on the aspect ratios of the expanding condensates are mainly for those containing  $N$  from 3000 to 9000. Working with such a small number of atoms, any fluctuation during each cycle of atom loading and cooling directly leads to atom number fluctuation. Normally, the number fluctuation  $\Delta N/N$  is  $\pm 10\%$  in these measurements. Our calculations show that a  $\pm 10\%$  jitter in atom number causes an aspect ratio uncertainty by

about  $\pm 0.6\%$  for the free expansion times of 10 to 20 milliseconds. We, on average, take 4 to 8 images of BEC clouds with certain atom numbers, under each trapping condition. To a good approximation each image of the BEC cloud is fitted by the Gaussian function along the radial and axial directions of the trap. The sizes ( $1/e$  radius)  $W_r$  and  $W_z$  of the condensate at different expansion times are directly extracted from the fitted curves.

However, image distortion is hard to completely eliminate during the probe time using the destructive absorption method. The dominant sources that affect the cloud size measurement are mainly from the lensing effect, probe beam heating, and image elongation due to gravitational acceleration. We now go to the details for each of these effects.

A small and dense atom cloud behaves like a lens of short focal length [24]. Depending upon the cloud density, size, imaging system, and probe laser detuning to the atomic resonance frequency, the lensing effect will cause different degrees of image distortion [25]. Our probe laser is locked on the atomic transition with a frequency jitter  $< 2$  MHz. To eliminate the residual lensing effect which degrades the cloud images, especially for a small condensate, we thus take the images only with expansion times longer than 11 ms. For those long expanded clouds their spatial densities are low enough that the lensing effect is not an issue any more.

We use a two-level atom model to estimate how much the cloud size increases from the heating effect while the atoms are exposed to the near-resonant photons during the probe time period. We assume each atom obtains a photon recoil kick after a cycle of absorption and emission of a photon from the probe laser. Since the photon reemission is isotropic if no other condition should be considered the probe beam thus causes cloud inflating equally in all directions. This also influences the aspect ratio measurements. For a cloud if its initial size,  $1/e$  radius, is  $W_0$ , after an exposure time  $t_p$  it expands to [26, 27]

$$W_{1/e} = \left(\frac{1}{t_p}\right) \int_0^{t_p} \sqrt{W_0^2 + \left(\frac{\hbar k}{m}\right)^2 \frac{1}{2} \frac{S}{1+S} \frac{t^3}{\tau}} dt, \quad (13)$$

with

$$S = \left(\frac{I}{I_s}\right) \frac{(\frac{\Gamma}{2})^2}{\Delta^2 + (\frac{\Gamma}{2})^2}, \quad (14)$$

where  $\Delta = \omega_L - \omega_0$  is the detuning of the laser frequency  $\omega_L$  to the atomic resonance frequency  $\omega_0$  and  $\tau = \frac{1}{\Gamma}$  is the lifetime of the excited state of the two-level atoms. The probe beam used for the measurements has a frequency close to the atomic resonance and an intensity  $I \sim 0.1I_s$ . Calculations using Eq. (14) show that the cloud size will increase by  $\sim 3.5\%$  and  $7.5\%$  when the probe pulse is  $100 \mu\text{s}$  and  $150 \mu\text{s}$ , respectively. We then equally correct the size in all directions to obtain the true cloud aspect ratio according to their measured sizes at different expansion times.

Photon recoil heating is an isotropic effect on the atomic size distortion. However, the center of mass acceleration of a cloud only occurs in the direction along the gravitational force. The cloud image taken at each expansion time  $t$  is indeed an integration of a series of atomic distribution profiles, falling at a center-of-mass speed of  $gt'$  at any instantaneous

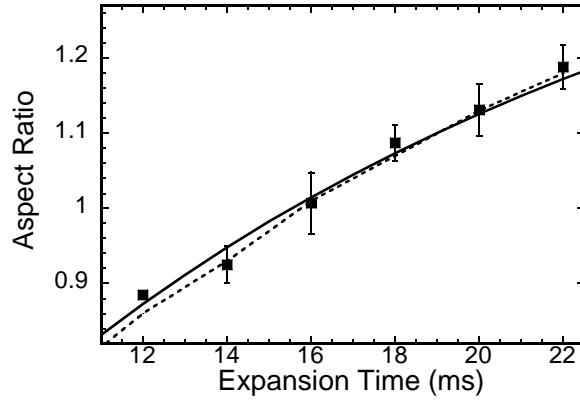


FIG. 3: Aspect ratio of the freely expanding condensate as a function of time for  $N = 9000$  and  $\omega_r = 2\pi \times 13.9$  Hz. The solid squares represent the experimental data, which are corrected for the gravity-induced elongation along the vertical direction and the heating effect from the probe photons. The probe time in this measurement is  $150 \mu\text{s}$ . The solid curve is calculated from the TF model using Eq. (10). The short-dashed curve shows the numerical solution.

time  $t'$ , through a period from  $t$  to  $t + t_p$ . The extent that the cloud image elongates along the gravity direction depends on the true cloud size and the probe time duration. Our calculations for  $N = 3000$  to  $9000$  show that the gravitational acceleration increases the cloud size by about 6% and 10% during the probe periods of  $100 \mu\text{s}$  and  $150 \mu\text{s}$ , respectively [28].

Fig. 3 shows the experimental data for the condensate aspect ratio measurement at  $N=9000$  and  $\omega_r = 2\pi \times 13.9$  Hz. The measured data lie well on the two theoretical curves calculated by using the Thomas-Fermi approximation and with the direct numerical solutions of the GP equation. This measurement indicates that a condensate at a trapping frequency of 13.9 Hz containing atom number  $N \geq 15$  ( $\frac{a_{ho}}{a}$ ), as shown in Eq. (5), is suitably described by the TF approximation.

To verify that the condensates gradually deviate from the TF regime, we do the aspect ratio measurements by lowering the atom number  $N$  from 5500 to 3000 and adjusting the trap radial trap frequency  $\omega_r$  to two different values,  $2\pi \times 12.19$  Hz and  $2\pi \times 13.9$  Hz. The experimental results are plotted in Fig. 4(a) to Fig. 4(d), respectively. The data indicate that, as  $N < 15$  ( $\frac{a_{ho}}{a}$ ), the time-dependent aspect ratio  $\sigma(t)$  deviates from the TF approximation curve gradually as  $N$  becomes smaller, though the measured data still lie reasonably well on the numerically solved curves.

To quantitatively show the transition from the TF regime to beyond the TF regime, we define the aspect ratio deviation from the TF model as  $\Delta\sigma(t)/\sigma^{TF}(t) = [\sigma(t) - \sigma^{TF}(t)]/\sigma^{TF}(t)$ , where  $\sigma^{TF}(t)$  is the aspect ratio at time  $t$  obtained from the TF model and  $\sigma(t)$  is from the measurements or calculations by the numerical method. For each  $N$  the mean aspect ratio deviation  $\langle \Delta\sigma/\sigma^{TF} \rangle$  is defined as the average of deviations  $\Delta\sigma(t)/\sigma^{TF}(t)$  over the expansion time  $t$  from 12 to 20 milliseconds.

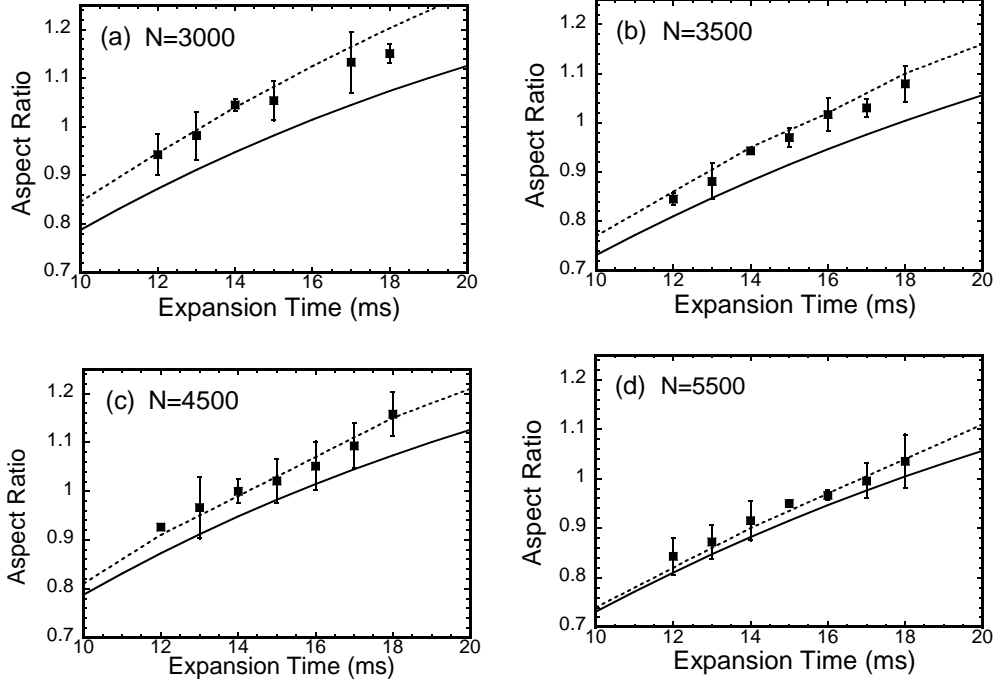


FIG. 4: Aspect ratio of the freely expanding condensate as a function of time. (a) and (c) represent the measurements at the radial trap frequency  $\omega_r = 2\pi \times 13.9$  Hz for  $N = 3000$  and  $4500$ , respectively. (b) and (d) represent the measurements at the radial trap frequency  $\omega_r = 2\pi \times 12.19$  Hz for  $N = 3500$  and  $5500$ , respectively. In all plots, the solid curves are calculated from the TF model. The solid squares represent the experimental data. The short-dashed curves show the numerical solutions. The probe time in these measurements is  $100 \mu\text{s}$ . All the data are also corrected for the gravity-induced elongation in the vertical direction and the heating effect from the probe photons.

We plot  $\langle \Delta\sigma/\sigma^{TF} \rangle$  versus  $N$  in Fig. 5. When the atom number  $N$  is 9000 the mean aspect ratio deviations from the TF model are less than 0.3% for both the measured data and the numerical solutions. The mean deviation becomes larger as  $N$  is lowered. When  $N=3000$ , the mean deviation from the experimental data is  $\sim 8.2\%$  and  $\sim 10.9\%$  from the numerical method. We believe the small discrepancy between our data and the numerical solutions, especially when  $N < 5000$ , is mainly due to the small absorption signal which is limited by the atom number and CCD sensitivity. However, from this figure, the transition from a TF regime to the regime beyond the TF model is clearly observed.

In conclusion, we have measured the aspect ratio of the freely expanded  $^{87}\text{Rb}$  condensates released from a magnetic TOP trap. Under our trapping conditions, we observe the transition regime where the condensate aspect ratio starts to deviate from the predictions of the Thomas-Fermi model when the atom number is gradually lowered from 9000 to 3000. Our measurements show a reasonable agreement with the numerical calculations and allow us to experimentally verify the lower bound of atom numbers required for applying the TF

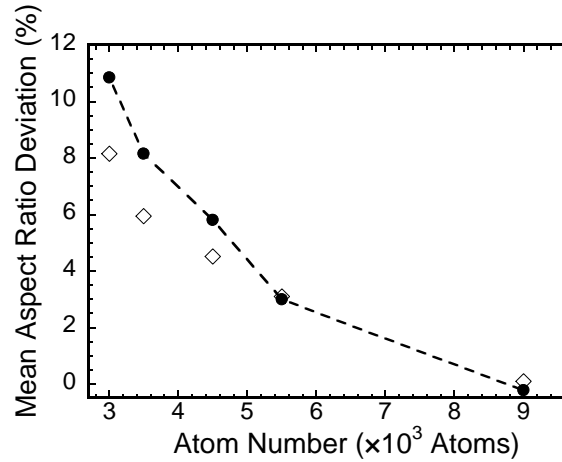


FIG. 5: Mean aspect ratio deviation as a function of atom number  $N$ . The empty diamonds show the mean deviations for the experimental data. The solid circles represent the mean deviations for the aspect ratios solved by the numerical method.

approximation on the  $^{87}\text{Rb}$  Bose-Einstein condensates.

## Acknowledgments

We are grateful to Y. C. Lang for the assistance during the early stage of this experiment. This work was supported by the National Science Council of R.O.C. under NSC grant NO. 92-2112-M-194-019.

## References

- \* Electronic address: [phydjh@ccu.edu.tw](mailto:phydjh@ccu.edu.tw)
- [1] M. H. Anderson, J. R. Ensher, M. R. Matthews, C. E. Wieman, and E. A. Cornell, *Science* **269**, 198 (1995).
  - [2] K. B. Davis, M. O. Mewes, M. R. Andrews, N. J. van Druten, D. S. Durfee, D. M. Kurn, and W. Ketterle, *Phys. Rev. Lett.* **75**, 3969 (1995).
  - [3] C. C. Bradley, C. A. Sackett, J. J. Tollett, and R. G. Hulet, *Phys. Rev. Lett.* **75**, 1687 (1995).
  - [4] For a recent review of the theory and experimental works, see, e.g. Legget *Rev. Mod. Phys.* **73**, 307 (2001). For a recent BEC works, see also the following web sites: <http://amo.phy.gasou.edu/bec.html>; <http://jilawww.colorado.edu/bec/> and references therein.
  - [5] L. P. Pitaevskii, *Zh. Eksp. Theor. Fiz.* **40**, 646 (1961) [*Sov. Phys. JETP* **13**, 451 (1961)]; E. P. Gross, *Nuovo Cimento* **20**, 454 (1961).
  - [6] D. S. Jin, J. R. Ensher, M. R. Matthews, C. E. Wieman, and E. A. Cornell, *Phys. Rev. Lett.* **77**, 420 (1996).
  - [7] M. -O. Mewes, M. R. Andrews, N. J. van Druten, D. M. Kurn, D. S. Durfee, C. G. Townsend,

- and W. Ketterle, Phys. Rev. Lett. **77**, 988 (1996).
- [8] K. W. Madison, F. Chevy, W. Wohlleben, and J. Dalibard, Phys. Rev. Lett. **84**, 806 (2000).
  - [9] M. R. Andrews, D. M. Kurn, H. -J. Miesner, D. S. Durfee, C. G. Townsend, S. Inouye, and W. Ketterle, Phys. Rev. Lett. **79**, 553 (1997).
  - [10] W. Petrich, M. H. Anderson, J. R. Ensher, and E. A. Cornell, Phys. Rev. Lett. **74**, 3352 (1995).
  - [11] U. Ernst, A. Marte, F. Schreck, J. Shuster, and G. Rempe, Europhys. Lett. **41**, 1 (1998).
  - [12] U. Ernst, J. Shuster, F. Schreck, A. Marte, A. Kuhn, and G. Rempe, Appl. Phys. B **76**, 719 (1998).
  - [13] E. Hodby, G. Hechenblaikner, O. M. Marago, J. Arlt, S. Hopkins, and C. J. Foot, J. Phys. B: At. Mol. Opt. Phys. **33**, 4087 (2000).
  - [14] J. H. Müller, D. Ciampini, O. Morsch, G. Smirne, M. Fazzi, P. Verkerk, F. Fuso, and E. Arimondo, J. Phys. B: At. Mol. Opt. Phys. **33**, 4095 (2000).
  - [15] A. Gorlitz, J. M. Vogels, A. E. Leanhardt, C. Raman, T. L. Gustavson, J.R. Abo-Shaeer, A.P. Chikkatur, S. Gupta, S. Inouye, T. P. Rosenband, and W. Ketterle, Phys. Rev. Lett. **87**, 130402 (2001).
  - [16] P. A. Rupprecht, M. J. Holland, K. Burnett, and M. Edwards, Phys. Rev. A **51**, 4704 (1995).
  - [17] M. Holland and J. Cooper, Phys. Rev. A **53**, R1954 (1996).
  - [18] G. Baym and C. J. Pethick, Phys. Rev. Lett. **76**, 6 (1996).
  - [19] C. J. Foot, *Atomic Physics*, Oxford University Press, (2005).
  - [20] J. R. Gardner, R. A. Cline, J. D. Miller, D. J. Heinzen, H. M. J. M. Boesten, and B. J. Verhaar, Phys. Rev. Lett. **74**, 3764, (1995).
  - [21] Y. Castin and K. Dum, Phys. Rev. Lett. **77**, 3276 (1996).
  - [22] D. J. Han, Physics Bimonthly of the Physical Society of R.O.C. **27**, 384 (2005).
  - [23] Jason R. Ensher, Ph. D. Thesis, University of Colorado (1998).
  - [24] M. R. Andrews, M. -O. Mewes, N. J. van Druten, D. S. Durfee, D. M. Kurn, and W. Ketterle, Science **84**, 273 (1996).
  - [25] Michael R. Matthews, Ph. D. Thesis, University of Colorado (1998).
  - [26] Christopher R. Monroe, Ph. D. Thesis, University of Colorado (1992).
  - [27] M. T. DePue, S. L. Winoto, D. J. Han, and D. S. Weiss, Optics Communications **180**, 73 (2000).
  - [28] To model the gravity-induced elongation of the cloud size, we simply sum  $N$  equally displaced Gaussian distributed functions of  $1/e$  radius  $W$ . If the probe time is  $t_p$  at expansion time  $t$ , each Gaussian function is displaced in the gravity direction by  $\sim gt \times (t_p/N)$ . The integrated function is still Gaussian and has a  $1/e$  radius  $W'$ . The original cloud size  $W$  can be obtained from the integrated size  $W'$  which is recorded by the CCD camera.